Title

Pharmacological chaperone for α-crystallin partially restores transparency in cataract models

Permalink

Journal

ISSN

Authors

Makley, Leah N
McMenimen, Kathryn A
DeVree, Brian T
et al.

Publication Date

DOI

Peer reviewed

Pharmacological Chaperone for Alpha-Crystallin Partially Restores Transparency in Cataract Models

Leah N. Makley[1,†], **Kathryn A. McMenimen**[1,†], **Brian T. DeVree**[3], **Joshua W. Goldman**[2], **Brittney N. McGlasson**[2], **Ponni Rajagopal**[4], **Bryan M. Dunyak**[1], **Thomas J. McQuade**[5], **Andrea D. Thompson**[1], **Roger Sunahara**[3], **Rachel E. Klevit**[4], **Usha P. Andley**[2,*], and **Jason E. Gestwicki**[1,5,*]

[1]Departments of Pathology, Biological Chemistry and Medicinal Chemistry and the Life Sciences Institute, University of Michigan, Ann Arbor, MI

[2]Department of Ophthalmology and Visual Sciences, Washington University School of Medicine, St. Louis, MO

[3]Department of Pharmacology, University of Michigan, Ann Arbor, MI

[4]Department of Biochemistry, University of Washington, Seattle, WA

[5]Center for Chemical Genomics, University of Michigan, Ann Arbor, MI

Abstract

Cataracts reduce vision in 50% of individuals over 70 years of age and are a common form of blindness worldwide. Cataracts are caused when damage to the major lens crystallin proteins causes their misfolding and aggregation into insoluble amyloids. Using a thermal stability assay, we identified a class of molecules that bind α-crystallins (cryAA and cryAB) and reversed their aggregation *in vitro*. The most promising compound improved lens transparency in the R49C cryAA and R120G cryAB mouse models of hereditary cataract. It also partially restored solubility in aged mouse and human lenses. These findings suggest an approach to treating cataracts by stabilizing α-crystallins.

The mammalian lens grows by terminal differentiation of epithelial cells into elongated fiber cells. Protein synthesis and turnover in the mature fiber cell are halted, such that the proteins of the lens must remain soluble and transparent throughout life. This remarkable feat is accomplished, in part, by αA-crystallin (cryAA) and αB-crystallin (cryAB), which are molecular chaperones that belong to a family of small heat shock proteins (sHSPs) (1, 2). Together, cryAA and cryAB comprise 30% of the protein content of the lens, where they

*Correspondence can be addressed to: Jason E. Gestwicki, Ph.D., University of California at San Francisco, Department of Pharmaceutical Chemistry, Sandler Neuroscience Center, 675 Nelson Rising Lane, San Francisco, CA 94158, Ph. 415 502 7121, jason.gestwicki@ucsf.edu; Usha Andley, Ph.D., Washington University, Department of Ophthalmology and Visual Sciences, 660 S. Euclid Ave, Box 9086, St Louis, MO 63110, Ph. 314-362-7167, andley@vision.wustl.edu.
†These authors contributed equally

help maintain the solubility of the other lens proteins, such as β- and γ-crystallins (2). Accumulated damage to these proteins over an individual's lifetime can lead to age-related nuclear cataracts, which are composed of aggregated crystallin proteins (3) (2, 4–6). Clues to the mechanism(s) of age-associated cataracts come from hereditary forms of the disease, which are caused by mutations, such as R120G cryAB, that destabilize the lens proteins (7). For example, the R120G mutation disrupts ionic interactions that normally stabilize the cryAB dimer (Fig S1A). It is thought that the unstable protein then assembles into amyloid-like fibers, forming a physical barrier to light and also, for the case of cryAA or cryAB, reducing the available chaperone activity in the lens. Thus, one potential way to treat cataracts may be to identify molecules that bind and stabilize crystallins, favoring the soluble, native forms (8).

Pharmacological chaperones (PCs) are small molecules that bind and stabilize a native state of a protein (9). A PC has been approved for clinical use in the treatment of transthyretin amyloidosis (10) and other PCs are being explored in late-stage clinical trials for use in treating a number of other misfolding diseases, such as Gaucher disease (11) and Anderson-Fabry disease (12). In the current work, we wanted to identify PCs that stabilize the soluble forms of cryAB to suppress its aggregation. Unlike previous targets for PC discovery (11), cryAB lacks natural substrates that are suitable as a starting point for drug design (13). Moreover, cryAB has no enzymatic activity, making it more difficult to envision a convenient high-throughput screen (HTS) strategy (10). These features place cryAB in a family of disease-associated proteins, including tau, myocilin, α-synuclein and huntingtin, which are often considered to be "undruggable" (14, 15).

We wondered whether differential scanning fluorimetry (DSF) might provide a way to circumvent some of these challenges. In a typical DSF experiment, an apparent melting transition (T_m) of the protein target is measured in the presence of potential ligands (16). Binding of a ligand usually adds free energy to the state that it binds, shifting the apparent T_m. DSF has been used for decades in biochemical studies, but has only recently been adapted for high-throughput (15, 17–19). To see if high throughput DSF might be applicable to the discovery of PCs for cryAB, we first purified recombinant human R120G cryAB and wild type cryAB and confirmed that both proteins were soluble and non-aggregated in solution (Fig S1B) (20). Upon gentle heating, R120G cryAB formed amyloids more readily than wild type cryAB, as measured by light scattering and electron microscopy (EM) (Figs 1Aa and 1Ab). Because amyloids are relatively heat-resistant structures, we suspected that samples of R120G cryAB might be more difficult to melt. To investigate this possibility, R120G cryAB and wild type cryAB were heated in the ThermoFluor® DSF platform. Consistent with the model, the apparent T_m of wild type cryAB was 64.1 ± 0.5 °C, whereas the T_m of the R120G cryAB mutant was 68.3 ± 0.2 °C (Fig 1Ac). Based on these observations, we hypothesized that molecules able to reduce the apparent T_m of R120G cryAB might be good candidates.

For the pilot screens, we turned to the model protein, Hsp27. Hsp27 was used because, while it retains the highly conserved crystallin domain found in cryAA and cryAB (Fig S1C), we found that it had a relatively high melting transition (T_m = 72 °C by three independent biophysical methods; Fig S1D). This feature provided a superior signal:noise in the high

throughput DSF platform, with Z' factor values between 0.5 and 0.8 and an average coefficient of variation (CV) of 8% at a final volume of only 7 μL in 384-well plates. Accordingly, we screened ~2,450 compounds from the MS2000 and NCC collections at a screening concentration between 20 and 40 μM. These compound collections include both natural and synthetic molecules that are known to have activity in a wide variety of assays. The primary screen identified 45 compounds (1.8%) that decreased the apparent T_m by at least three standard deviations ($\pm$ 0.6 °C) (Fig 1B). All 45 of these "actives" were explored in dose dependence experiments, revealing 32 (71%; 1.3% overall) that decreased the T_m at half-maximal concentrations less than 20 μM. Strikingly, twelve of the 32 confirmed actives belonged to a single class of related sterols, so we selected this scaffold for further investigation. Interestingly, one of the weakly active sterols was lanosterol. While this manuscript was under re-review, Zhao *et al.* reported that lanosterol has anti-cataract activity (21). However, this compound has limited solubility and it was only weakly active by HT-DSF, which inspired us to collect 32 additional sterols similar to compound **1** and screen them against R120G cryAB using the DSF procedure. Two compounds (**28**; 5a-cholestan-3b-ol-6-one and **29**;5-cholesten-3b,25-diol) were at least 2- to 3-fold more potent than sterol **1** (Fig. 1C), reducing the apparent T_m by at least 2 °C (Fig 1D, Fig S2A and Fig S2E). Many of the other sterols were inactive, suggesting a specific interaction. For example, compound **16** is structurally related to compounds **28** and **29** (Fig S2B), yet it was inactive (Fig 1D). To confirm the direct interaction of compound **29** with R120G cryAB, we used biolayer interferometry (BLI). Immobilized R120G cryAB bound to compound **29** with a K_D of 10.1 $\pm$ 4.4 μM (Figs. 1D, S2C and S2D), whereas compound **16** did not bind ($K_d >$ 50 μM). To examine where on R120G cryAB this interaction takes place, we used ^{15}N-HSQC NMR experiments to show that compound **29**, but not compound **16**, bound to the crystallin domain at the dimer interface (Fig S3A–C). Based on the chemical shift perturbations (CSPs), we docked compound **29** to cryAB, revealing that this compound fits into a groove that lies between the two protomers (Fig 2B). In this configuration, compound **29** is predicted to make contacts with both cryAB subunits, suggesting that it might stabilize the native state.

To test whether compound **29** might block amyloid formation, we treated R120G cryAB (15 μM) with compounds **29** or **16** (100 μM) and the extent of aggregation was examined by electron microscopy (EM). These studies confirmed that compound **29**, but not **16** or the vehicle control, partially suppressed amyloid formation when added prior to the initiation of aggregation (Fig. 2A). To test whether **29** might also have an effect on pre-formed aggregates, we pre-generated R120G cryAB amyloids and then treated them with compound **29** or **16**. Again, compound **29**, but not **16**, was able to partially reverse amyloid formation (Fig 2A). The reversal took approximately two days, suggesting a slow equilibrium between the amyloid and the soluble forms of cryAB. To quantify these activities, we again treated R120G cryAB with **29** or **16**, then separated the insoluble and soluble material by centrifugation and measured the amount of protein in these fractions using bicinchininic acid (BCA) assays. Consistent with the EM results, compound **29**, but not **16** or the vehicle control, shifted cryAB into the soluble fraction when added either before or after aggregation (Fig 2A). Together, these results show that compound **29** can block aggregation and partially reverse R120G cryAB insolubility *in vitro*. To test if this activity was restricted

to the R120G model, we next used the DSF platform to test whether compound **29** could restore the solubility of other cataract-associated protein. We found that compound **29** could improve the T_m of three mutants in cryAA (R49C, F71L and R116C) by at least 2 °C (Fig S4). This effect might be expected because cryAA and cryAB are highly conserved, especially in the region that binds compound **29** (see Fig S1C). However, compound **29** had no effect on two mutants of the structurally unrelated lens protein, γ-crystallin (P23T or W42R cryAG) (Fig S4), which lacks the crystallin domain. Thus, compound **29** appears to bind a specific region of cryAA and cryAB to restore solubility and partially reverse aggregation.

The R120G cryAB knock-in mouse develops severe age-associated cataracts, with 100% showing lens opacities by 20 weeks of age (22). To test whether compound **29** can reverse this process, a single drop of compound **29** or vehicle (cyclodextrin) was delivered to the right eye of aged R120G cryAB knock-in mice three times per week for two weeks. These mice had already developed severe cataracts prior to the treatments. Lens opacity was then assessed with a video slit lamp and scored using a five-grade scale adapted from the LOCS III cataract scoring system. In heterozygous R120G cryAB mice (age 36 to 366 days), we observed a striking improvement in lens opacity grade (lens opacity grade 0.98 ± 0.46; N=22; p <0.001) (Fig 2C). Importantly, compound **16**, was inactive (lens opacity grade 2 ± 0; N=3; p > 0.2). The effect of compound **29** was striking by visual inspection (Fig. 2C), quantification of the pixel intensities (Fig 2C) or quantitative reconstructions of the slit lamp videos (Fig S5). To examine the durability of this effect, we examined the mice four weeks after ending treatment with compound **29**. In these mice, the LOCS III cataract score was indistinguishable from the values taken immediately after treatment (lens opacity grade ~1.0). The cataracts in R120G cryAB mice become more dramatic with age. To test whether compound **29** could act on these cataracts, a second group of older heterozygotes was treated with a 1 mM solution three times per week for two weeks, revealing that lens opacity was significantly improved (lens opacity grade 1.25 ± 0.46; N=10; p<0.001) (Fig 2B). Thus, compound **29** could even partially restore the transparency of older cryAB R120G heterozygous mice.

The R49C cryAA heterozygous knock-in mouse also develops cataracts. To investigate the effect of compound **29** on this second model of hereditary cataract, we treated mice with 5 mM compound **29** or vehicle control three times per week for four weeks. We found that the lens transparency was significantly increased (lens opacity grade 1.11 ± 0.72; N=14; p<0.001) (Fig. S6A). Similarly, a second group of R49C cryAA heterozygotes was treated with a lower dose (1 mM solution of compound **29**) three times per week for two weeks, showing similar efficacy (lens opacity grade 1.3 ± 0.51; N=5; p=0.006) (Fig. S6A). Thus, compound **29** could partially restore transparency to two distinct models of hereditary cataract.

Although cataracts and the amount of total insoluble lens protein are only indirectly related (1), an improvement in overall protein solubility might be expected for compounds that have a striking anti-aggregation activity. To test whether compound **29** could restore protein solubility, we separated the soluble and insoluble fractions of treated lenses by centrifugation and measured the amount of crystallins (α, β and γ) by gel permeation

chromatography (GPC). We found that compound **29** improved the solubility of the α-crystallins (including cryAA and cryAB) by 63% (S6B). Moreover, the shape of this curve was similar to the untreated α-crystallins, suggesting that compound **29** favors a normal structure of the proteins. To verify this finding using a different method, we measured the total amount of soluble and insoluble protein in a subset of the treated lenses by BCA assays. Consistent with this model, compound **29** increased the ratio of soluble:insoluble protein by $16 \pm 5\%$ (Fig. 2C). Again, older heterozygous mice showed a more robust response (Fig S6C).

Hereditary cataracts are relatively rare in humans, so we next explored whether compound **29** might have an effect on the more prevalent, age-related cataracts. The exact mechanisms of age-associated cataracts are not clear, but likely involve oxidative and other damage to crystallin proteins, resulting in aggregation. Five C57BL/6J wild type mice (aged 118 to 263 days) with spontaneous, age-associated opacities were treated with compound **29** for two weeks and then examined by slit lamp biomicroscopy. We found that compound **29**, but not vehicle control, improved transparency by at least 1 grade on the LOCS III scoring system in four of the five mice. Finally, we collected lens material from human patients (aged 70 to 80 years) with grade 1 to 4 cataracts and treated them with either vehicle or compound **29** for six days *ex vivo*. Compound **29**, but not the vehicle, significantly improved the amount of soluble protein by 18%, as assessed by BCA assays (Fig 2C and S6D). Thus, compound **29** may be a promising lead towards the non-surgical treatment of both hereditary and age-associated cataracts. This molecule partially reversed protein aggregation by binding and stabilizing the more soluble forms of cryAA and cryAB, suggesting that it is a pharmacological chaperone (PC) for these crystallins. Based on the *in vitro*, *in vivo* and *ex vivo* studies, we suggest that compound **29** stabilizes the native forms of cryAB, which are in slow equilibrium with the amyloid forms. Once stabilized, the bound cryAB is less now likely to misfold, a key feature of a PC. The SEC results also suggest that the treated cryAB is now partly capable of keeping other lens crystallin proteins soluble, suggesting that its chaperone activity is at least partially intact. Finally, and more broadly, these findings suggest that DSF-based HTS campaigns might be ideally suited for identifying PCs with activity against other "undruggable" targets.

Supplementary Material

Refer to Web version on PubMed Central for supplementary material.

Acknowledgments

References

1. Bloemendal H, et al. Ageing and vision: structure, stability and function of lens crystallins. Prog Biophys Mol Biol. Nov.2004 86:407. [PubMed: 15302206]

2. Haslbeck M, Franzmann T, Weinfurtner D, Buchner J. Some like it hot: the structure and function of small heat-shock proteins. Nat Struct Mol Biol. Oct.2005 12:842. [PubMed: 16205709]

3. Leibowitz HM, et al. The Framingham Eye Study monograph: An ophthalmological and epidemiological study of cataract, glaucoma, diabetic retinopathy, macular degeneration, and visual acuity in a general population of 2631 adults, 1973–1975. Survey Ophthalmol. May-Jun;1980 24:335.

4. Meehan S, et al. Amyloid fibril formation by lens crystallin proteins and its implications for cataract formation. J Biol Chem. Jan 30.2004 279:3413. [PubMed: 14615485]

5. Meehan S, et al. Characterisation of amyloid fibril formation by small heat-shock chaperone proteins human alphaA-, alphaB- and R120G alphaB-crystallins. J Mol Biol. Sep 14.2007 372:470. [PubMed: 17662998]

6. Pande A, et al. Crystal cataracts: human genetic cataract caused by protein crystallization. Proc Natl Acad Sci U S A. May 22.2001 98:6116. [PubMed: 11371638]

7. Vicart P, et al. A missense mutation in the alphaB-crystallin chaperone gene causes a desmin-related myopathy. Nat Genet. Sep.1998 20:92. [PubMed: 9731540]

8. Moreau KL, King JA. Protein misfolding and aggregation in cataract disease and prospects for prevention. Trends Mol Med. May.2012 18:273. [PubMed: 22520268]

9. Cohen FE, Kelly JW. Therapeutic approaches to protein-misfolding diseases. Nature. Dec 18.2003 426:905. [PubMed: 14685252]

10. Hammarstrom P, Wiseman RL, Powers ET, Kelly JW. Prevention of transthyretin amyloid disease by changing protein misfolding energetics. Science. Jan 31.2003 299:713. [PubMed: 12560553]

11. Sawkar AR, D'Haeze W, Kelly JW. Therapeutic strategies to ameliorate lysosomal storage disorders–a focus on Gaucher disease. Cell Mol Life Sci. May.2006 63:1179. [PubMed: 16568247]

12. Fan JQ, Ishii S. Active-site-specific chaperone therapy for Fabry disease. Yin and Yang of enzyme inhibitors. FEBS J. Oct.2007 274:4962. [PubMed: 17894781]

13. Biswas A, Das KP. Role of ATP on the interaction of alpha-crystallin with its substrates and its implications for the molecular chaperone function. J Biol Chem. Oct 8.2004 279:42648. [PubMed: 15292216]

14. Makley LN, Gestwicki JE. Expanding the number of 'druggable' targets: non-enzymes and protein-protein interactions. Chem Biol Drug Design. Jan.2013 81:22.

15. Burns JN, et al. Rescue of glaucoma-causing mutant myocilin thermal stability by chemical chaperones. ACS Chem Biol. May 21.2010 5:477. [PubMed: 20334347]

16. Cummings MD, Farnum MA, Nelen MI. Universal screening methods and applications of ThermoFluor. J Biomol Screen. Oct.2006 11:854. [PubMed: 16943390]

17. Fedorov O, Niesen FH, Knapp S. Kinase inhibitor selectivity profiling using differential scanning fluorimetry. Methods Mol Biol. 2012; 795:109. [PubMed: 21960218]

18. Major LL, Smith TK. Screening the MayBridge Rule of 3 Fragment Library for Compounds That Interact with the Trypanosoma brucei myo-Inositol-3-Phosphate Synthase and/or Show Trypanocidal Activity. Mol Biol International. 2011; 2011:389364.

19. Lavinder JJ, Hari SB, Sullivan BJ, Magliery TJ. High-throughput thermal scanning: a general, rapid dye-binding thermal shift screen for protein engineering. J Am Chem Soc. Mar 25.2009 131:3794. [PubMed: 19292479]

20. Materials and methods are available as supplementary materials on Science Online

21. Zhao L, et al. Lanosterol reverses protein aggregation in cataracts. Nature. Jul 30.2015 523:607. [PubMed: 26200341]

22. Andley UP, Hamilton PD, Ravi N, Weihl CC. A knock-in mouse model for the R120G mutation of alphaB-crystallin recapitulates human hereditary myopathy and cataracts. PLoS ONE. 2011; 6:e17671. [PubMed: 21445271]
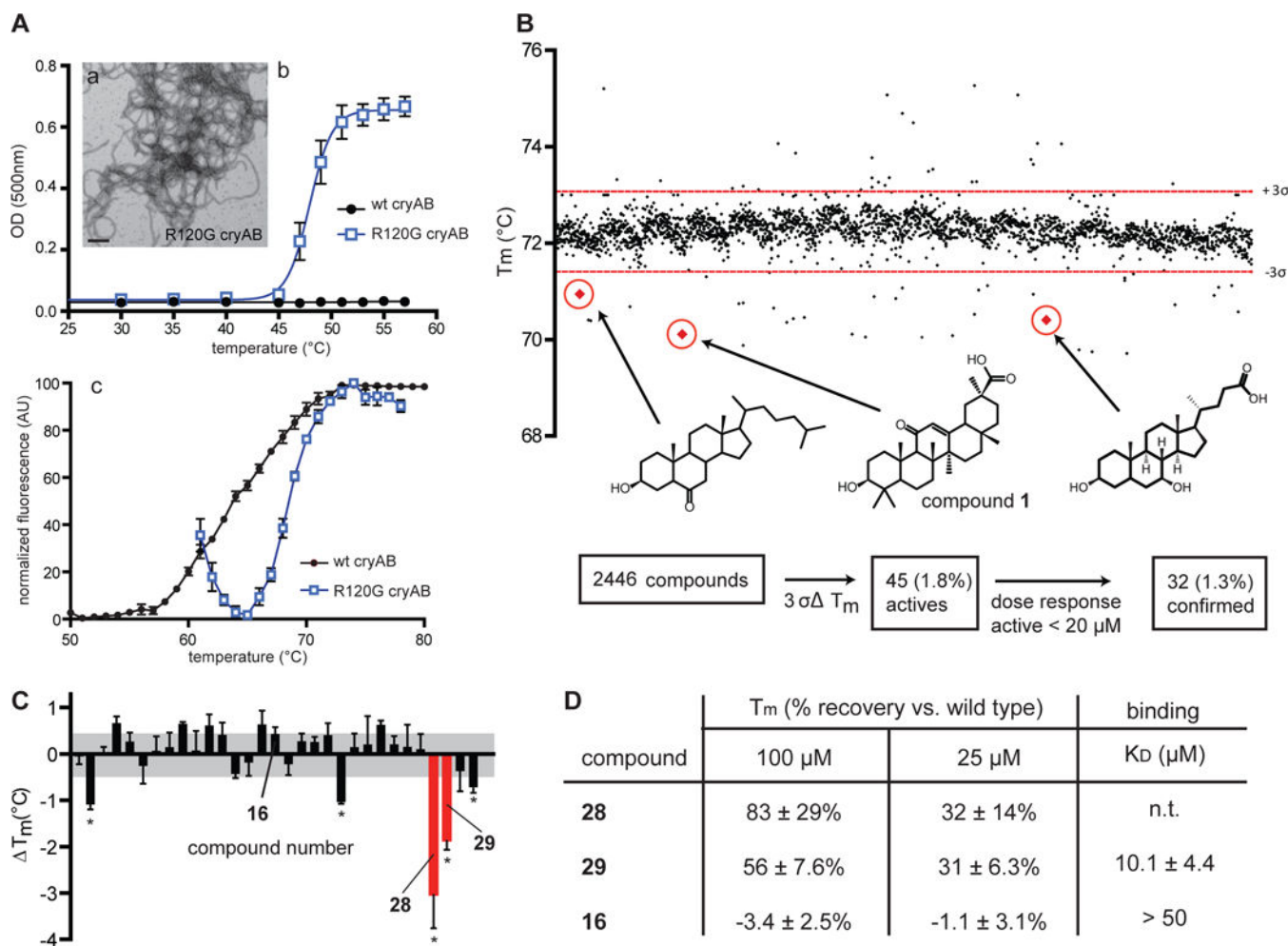
Fig 1. High throughput DSF screen identifies pharmacological chaperones for a small heat shock protein

(A) The R120G mutant of cryAB (blue) forms heat resistant amyloids, as judged by electron microscopy (a), light scattering (b) and DSF (c). Wild type cryAB (black) is more resistant to misfolding and has a lower melting transition by DSF, but will form amyloids under harsher conditions (Fig S1). Results are the average of triplicates and error bars represent SEM. Microscopy results are representative of studies on at least three independent samples. Scale bar is 0.25 μm. (B) Summary of DSF screen against Hsp27. The structures of three active sterols are shown. (C) A collection of 32 sterols, based on compound 1, were screened at 20 μM for the ability to restore the T_m of R120G cryAB. Compounds 28 and 29 were 2- to 3-fold more potent than the initial active molecule. (D) Compounds 28 and 29, but not the control compound 16, partially restored the T_m of R120G cryAB and bound to the protein. Results are the average of at least triplicates and error is SEM.
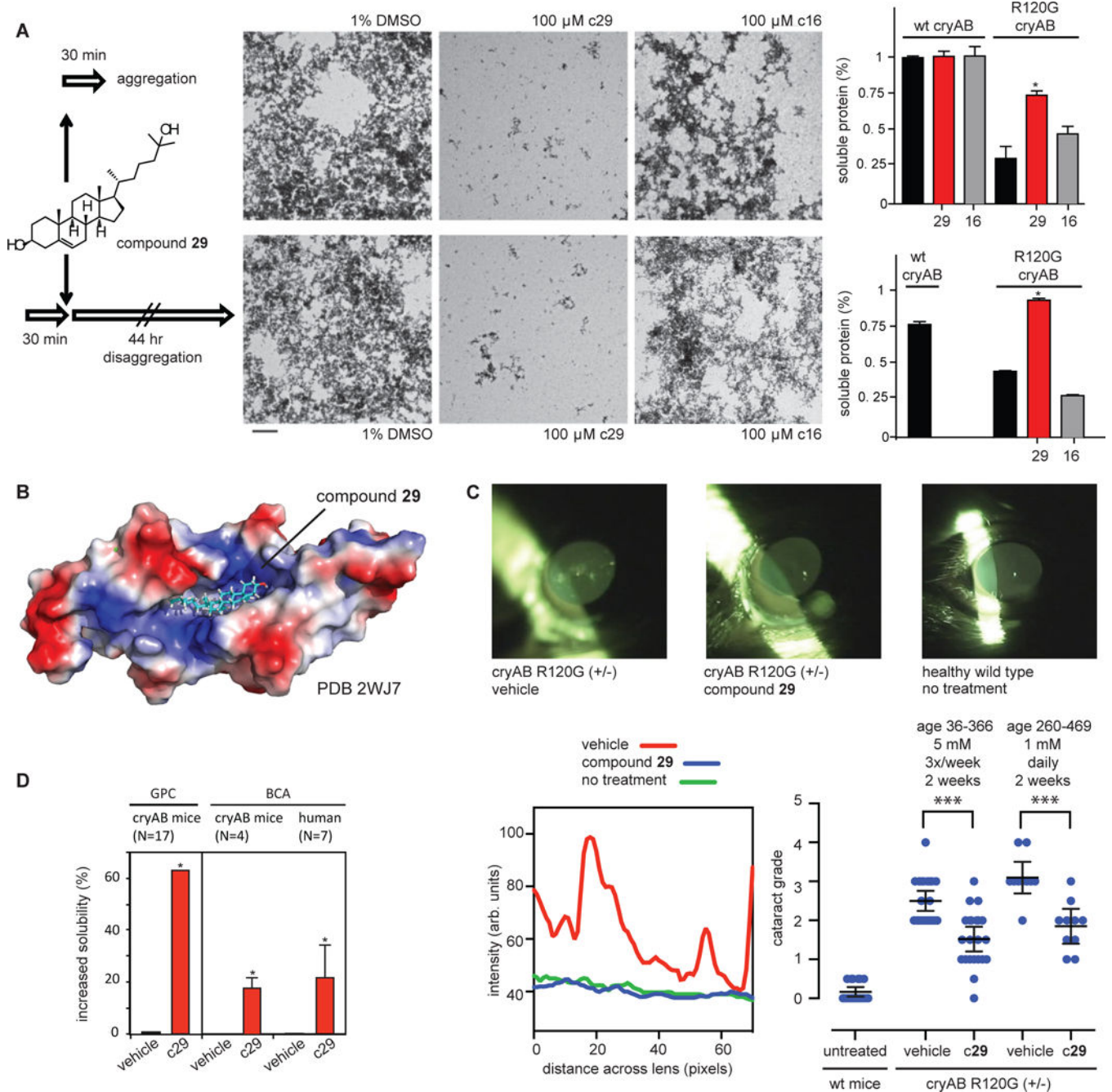
Fig 2. Compound 29 reverses cataract formation in vitro and in the R120G cryAB knock-in mouse

(A) Purified R120G cryAB (20 μM) was treated with compound 29 (100 μM), 16 (100 μM) or a DMSO control (1%) and then aggregated at ambient temperature with shaking for 30 minutes for the aggregation study. For the disaggregation study, amyloid fibrils were formed using the conditions above (40 μM) and then the samples were treated with 100 μM compound. Aliquots were visualized at 44 hours after treatment. Samples were visualized by electron microscopy and then centrifuged to remove insoluble material. The levels of soluble and insoluble R120G cryAB were assessed by absorbance at 280 nm. Results are the

average of independent triplicates and the error bars represent SEM. Electron micrographs are representative of independent triplicates. Scale bar is 1 μm. (B) Docking of compound 29 to the crystallin domain of cryAB, based on NMR titrations and chemical shift perturbations. See the Supplemental Material for details. (C) Summary of the treatment of R120G cryAB knock-in mice with compound 29. Slit lamp images and corresponding densitometry plots are shown for wild type mice aged 60–240 days; cryAB R120G heterozygotes aged 66–366 days, treated with vehicle control or 29 (5 mM) every other day for 2 weeks; cryAB R120G heterozygotes aged 260 days–469 days treated with vehicle or 29 (1 mM) daily for 2 weeks. The transparency of the treated mice was measured using a LOCS III scoring system on masked images. In both dosing schedules, 29 significantly improved transparency. $p < 0.001$. (D) Treatment with compound 29 improved the solubility of mouse and human lens proteins, as measured by BCA assays.